PHYSICAL REVIEW A VOLUME 40, NUMBER 12 DECEMBER 15, 1989

Theoretical and computer-simulation study of the density fluctuations in liquid water

M. A. Ricci
Dipartimento di Fisica, Università di L'Aquila, 68100 L'Aquila, Italy

D. Rocca
Dipartimento di Fisica, Università "La Sapienza," 00185 Roma, Italy

G. Ruocco
Dipartimento di Fisica, Università di L'Aquila, 68100 L'Aquila, Italy

R. Vallauri
Istituto di Elettronica Quantistica del Consiglio Nazionale delle Ricerche, 50127 Firenze, Italy
(Received 7 June 1989)

A theoretical and molecular dynamics analysis of hydrogen and oxygen density correlation functions in liquid water is presented with the aim of clarifying the present experimental situation. In the theoretical study, besides the ordinary sound mode, a high-frequency "optical-like" collective mode is found to propagate through the hydrogen atoms. The dispersion relation of the two modes is discussed. Computer-simulation results for the partial intermediate scattering functions are reported and confirm the theoretical predictions. The direct comparison of the theoretical predictions and the computer-simulation results with the experimental findings suggests an interpretation of the nature of the two modes. Finally the collective character of the propagating modes is pointed out by comparing the self-part of the scattering function with the total one.

I. INTRODUCTION

The study of the propagation of collective excitations of finite wave vectors in simple monatomic liquids has been the subject of numerous theoretical, molecular dynamics, and experimental investigations.[1] In fact the possible persistency of a sound mode with wavelength as short as an interatomic distance (i.e., well out of the hydrodynamic regime) is still a challenging open problem, underlying the correct physical interpretation of the coherent-neutron-scattering results. The connection between the experimental results and the microscopic quantities has been established in Van Hove's fundamental paper,[2] where it is shown how the coherent inelastic neutron scattering spectrum $S(k,\omega)$ is related to the density correlation functions of the system. A commonly adopted method to examine the data[3] is to report the frequency of the peaks of $\omega^2 S(k,\omega)$ as a function of the wave vector k (dispersion relation) and to compare it with the extrapolation of the hydrodynamic sound dispersion. Broadly speaking the behavior of the dispersion relation is characterized by a possible positive deviation from the short-wave-vector linear dispersion, always followed by a maximum and a subsequent minimum, occurring at a k value corresponding to the first peak of the structure factor $S(k)$.[1]

Computer simulations on well-defined model systems have widely been used as a valuable test of the theoretical approaches; in particular, they have been proved to be of overwhelming importance to understand the effect of the atomic interaction potential on the sound wave propagation in the same wave-vector range accessible to neutron scattering. Typical examples are the studies of hard spheres,[4] Lennard-Jones[5] (LJ), and metal-like systems.[6]

Instead much less attention has been devoted until now to the collective dynamical properties of molecular liquids. To our knowledge only two systems have been experimentally investigated, namely liquid parahydrogen, for which the coherent neutron scattering spectrum has been measured by Carneiro *et al.*,[7] and liquid water. The latter is, in any case, the system for which relatively more data have been reported both from the experimental[8,9] and computational[10–12] points of view. In this system a linear dispersion relation has been observed in the wave-vector range $0.3 < k < 1.5$ Å^{-1} both experimentally[9] and by computer simulation.[12] Because of the resulting high sound velocity (≈ 3200 m/s), the interpretation of the nature of this collective excitation is still matter of some controversy. The high sound velocity is explained by Teixeira *et al.*[9] as a manifestation of a new collective excitation ("fast sound") propagating in the small patches of highly bonded water molecules. On the contrary Wojcik and Clementi[12] claim a positive dispersion of the ordinary hydrodynamic mode to be the origin of such a behavior, thus extending to molecular systems the physical concepts invoked to account for similar (but less evident) results in monatomic liquids.

Recently we have presented the results of a theoretical analysis[13] of the dispersion relation in liquid water. While in previous papers only the center-of-mass density fluctuations were taken into account, in our analysis the density fluctuations of both the oxygen and hydrogen

atoms are considered in order to have a direct comparison with the neutron-scattering measurements. The analysis through a two-dimensional dynamical variable leads naturally to an additional mode, the nature of which has to be clarified.

In this paper we present the details of the theoretical analysis and deeply discuss the results for the dispersion relation. Moreover computer simulation data for the partial intermediate scattering functions are separately reported for the first time. The direct comparison of the theoretical predictions and the computer simulation results with the experimental findings suggests an interpretation of the nature of the two modes. This is also achieved by looking at the self-contribution to the scattering functions and its comparison with the total $S(k,\omega)$. The role of the interaction potential in determining the collective dynamical properties is also pointed out by stressing the differences between previous computer simulation and our results.

II. OUTLINE OF THE THEORY

In this section we present a theoretical analysis of the density fluctuations which leads to the prediction of two branches in the $\omega(k)$ dispersion relation, starting from the knowledge of the static properties of the system.

A. The projection operator formalism

Our analysis is based on the projection operator formalism developed by Mori and Zwanzig,[14] applied to a dynamical variable

$$\rho(\mathbf{r},t)=\begin{bmatrix}\rho^{(1)}(\mathbf{r},t)\\ \rho^{(2)}(\mathbf{r},t)\end{bmatrix} \tag{1}$$

whose components $\rho^{(1)}(\mathbf{r},t)$ and $\rho^{(2)}(\mathbf{r},t)$ represent the density fluctuations of the oxygen and hydrogen atoms respectively; i.e.,

$$\rho^{(1)}(\mathbf{r},t)=\left[\sum_i \delta(\mathbf{r}-\mathbf{R}_i^{(O)}(t))-N/V\right]\Big/\sqrt{N}\ , \tag{2a}$$

$$\rho^{(2)}(\mathbf{r},t)=\left[\sum_i[\delta(\mathbf{r}-\mathbf{R}_i^{(H(1))}(t)) +\delta(\mathbf{r}-\mathbf{R}_i^{(H(2))}(t))]-2N/V\right]\Big/\sqrt{N}\ , \tag{2b}$$

where N is the total number of molecules in the volume V; $\mathbf{R}_i^{(O)}(t)$, $\mathbf{R}_i^{(H(1))}(t)$, and $\mathbf{R}_i^{(H(2))}(t)$ represent the positions of the oxygen and the two hydrogen atoms of the molecule i respectively.

We are interested in the correlation function matrix $\underline{C}(k,t)$

$$\underline{C}(k,t)=\langle\rho_k(t)\cdot\rho_k^{\dagger}(0)\rangle =\begin{bmatrix}\langle\rho_k^{(1)}(t)\rho_{-k}^{(1)}(0)\rangle & \langle\rho_k^{(1)}(t)\rho_{-k}^{(2)}(0)\rangle\\ \langle\rho_k^{(2)}(t)\rho_{-k}^{(1)}(0)\rangle & \langle\rho_k^{(2)}(t)\rho_{-k}^{(2)}(0)\rangle\end{bmatrix}, \tag{3}$$

where the angular brackets indicate an ensemble average and the spatial Fourier transform of $\rho(\mathbf{r},t)$ is introduced

$$\rho_k(t)=\begin{bmatrix}\rho_k^{(1)}(t)\\ \rho_k^{(2)}(t)\end{bmatrix}, \tag{4}$$

i.e.,

$$\rho_k^{(1)}(t)=\left[\sum_i \exp[i\mathbf{k}\cdot\mathbf{R}_i^{(O)}(t)]-(2\pi)^3\delta(\mathbf{k})N/V\right]\Big/\sqrt{N} \tag{5a}$$

$$\rho_k^{(2)}(t)=\left[\sum_i\{\exp[i\mathbf{k}\cdot\mathbf{R}_i^{(H(1))}(t)]+\exp[i\mathbf{k}\cdot\mathbf{R}_i^{(H(2))}(t)]\} -2(2\pi)^3\delta(\mathbf{k})N/V\right]\Big/\sqrt{N}\ . \tag{5b}$$

At $t=0$ the correlation matrix in Eq. (3) reduces to

$$\underline{C}(k,0)=\begin{bmatrix}S_{11}(k) & 2S_{12}(k)\\ 2S_{12}(k) & 4S_{22}(k)\end{bmatrix}, \tag{6}$$

where $S_{\alpha\beta}(k)$ are the partial structure factors, which can be written as[15]

$$S_{11}(k)=1+\frac{N}{V}\int d\mathbf{r}\exp(i\mathbf{k}\cdot\mathbf{r})[g_{O\text{-}O}(r)-1]\ , \tag{7a}$$

$$S_{12}(k)=[\sin(kr_{12})/(kr_{12})] +\frac{N}{V}\int d\mathbf{r}\exp(i\mathbf{k}\cdot\mathbf{r})[g_{O\text{-}H}(r)-1]\ , \tag{7b}$$

$$S_{22}(k)=[1+\sin(kr_{22})/(kr_{22})]/2 +\frac{N}{V}\int d\mathbf{r}\exp(i\mathbf{k}\cdot\mathbf{r})[g_{H\text{-}H}(r)-1]\ . \tag{7c}$$

The three $g_{\alpha\text{-}\beta}(r)$ represent the intermolecular atom-atom distribution functions; r_{12} is the distance between an oxygen and hydrogen atom and r_{22} is the separation between the two hydrogen atoms belonging to the same molecule. A schematic representation of the water molecule is given in Fig. 1, in which the definition of all the used parameters is given. In the following we will deal with a rigid molecule, neglecting therefore the internal degrees of freedom.

The correlation function matrix $\underline{C}(k,t)$ turns out to obey the generalized Langevin equation

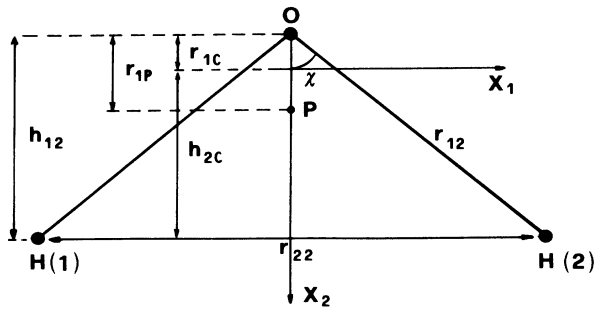

FIG. 1. Schematic representation of the water molecule. X_1 and X_2 are the in-plane principal axes. P indicates the site where the negative charge of the TIP4P potential model is placed. The values of the parameters are: $r_{22}=1.51$ Å, $h_{12}=0.586$ Å, $r_{12}=0.957$ Å, $r_{1P}=0.15$ Å.

$$\dot{\underline{C}}(k,t)=i\underline{\Omega}\cdot\underline{C}(k,t)-\int_0^t d\tau\underline{C}(k,t-\tau)\cdot\underline{M}(k,\tau)\ . \quad (8)$$

In our case the matrix elements of $\underline{\Omega}$, which are proportional to the cross correlation between the variable $\rho_k(t)$ and its time derivative $\dot{\rho}_k(t)$, are identically zero as demonstrated in Appendix A. The memory function matrix $\underline{M}(k,t)$ is written as

$$\underline{M}(k,t)=\langle\mathcal{F}(k,t)\cdot\mathcal{F}^{\dagger}(k,t)\rangle\langle\rho_k(0)\cdot\rho_k^{\dagger}(0)\rangle^{-1}\ , \quad (9)$$

where the fluctuating force $\mathcal{F}(k,t)$ is

$$\mathcal{F}(k,t)=\exp(iQ\mathcal{L}t)Q\dot{\rho}_k(t)\ . \quad (10)$$

$\mathcal{L}$ is the Liouville operator and $Q=1-P$, P being the projection operator over the dynamical variable $\rho_k(t)$. In turn $\underline{M}(k,t)$ satisfies the equation

$$\dot{\underline{M}}(k,t)=-\int_0^t d\tau\underline{M}(k,t-\tau)\cdot\underline{M}'(k,\tau)\ , \quad (11)$$

where $\underline{M}'(k,t)$ is the second-order memory function.

The solution of Eq. (8) is written for the Laplace transform of the correlation function matrix

$$\hat{\underline{C}}(k,z)=\int_0^{\infty} dt\exp(-zt)\underline{C}(k,t) \quad (12)$$

and reads

$$\hat{\underline{C}}(k,z)=\{z\underline{I}+[z\underline{I}+\underline{M}'(k,z)]^{-1}\cdot\underline{M}(k,0)\}^{-1}\cdot\underline{C}(k,0)\ , \quad (13)$$

where $\underline{I}$ is the unit tensor. If one is interested in looking only for the eigenmodes of the system, in a first approximation the damping can be neglected [i.e., $\underline{M}'(k,z)=0$] and Eq. (13) becomes

$$\hat{\underline{C}}(k,z)=[z\underline{I}+\underline{M}(k,0)/z]^{-1}\cdot\underline{C}(k,0)\ . \quad (14)$$

The eigenfrequencies are then found by solving the secular equation

$$\det[\underline{I}\omega^2-\underline{M}(k,0)]=0 \quad (15)$$

with $z=i\omega$. By using Eqs. (9) and (10) one has

$$\underline{M}(k,0)=\langle[Q\dot{\rho}_k(0)][Q\dot{\rho}_k(0)]^{+}\rangle\langle\rho_k(0)\cdot\rho_k^{\dagger}(0)\rangle^{-1}$$
$$=\langle\dot{\rho}_k(0)\cdot\dot{\rho}_k^{\dagger}(0)\rangle\langle\rho_k(0)\cdot\rho_k^{\dagger}(0)\rangle^{-1}\ . \quad (16)$$

A detailed calculation of the matrix elements which appear in Eq. (16) is reported in Appendix A. After straightforward algebra the secular Eq. (15) can be cast in the form

$$a(k)\omega^4-b(k)\omega^2+c(k)=0\ , \quad (17)$$

where

$$a(k)=S_{11}(k)S_{22}(k)-S_{12}^2(k)\ , \quad (18a)$$

$$b(k)=k^2[d_{11}(k)S_{22}(k)+d_{22}(k)S_{11}(k)-2d_{12}(k)S_{12}(k)]\ , \quad (18b)$$

$$c(k)=k^4[d_{11}(k)d_{22}(k)-d_{12}^2(k)]\ , \quad (18c)$$

with $S_{\alpha\beta}(k)$ given in Eqs. (7a)–(7c) and

$$d_{11}(k)=\frac{k_BT}{M}\{1+[MR_{1C}^2/(3I)]\}\ , \quad (19a)$$

$$d_{12}(k)=\frac{k_BT}{M}\{j_0(kr_{12})+[MR_{1C}h_{2C}/(3I)][j_0(kr_{12})+j_2(kr_{12})]-(MR_{1C}^2/I_3)(2h_{2C}/R_{1C}+1)j_2(kr_{12})\sin^2\chi\}\ , \quad (19b)$$

$$d_{22}(k)=\frac{k_BT}{M}\{[1+j_0(kr_{22})]/2+Mh_{2C}^2/(6I)[1+j_0(kr_{22})+j_2(kr_{22})]+Mr_{22}^2/(24I')[1-j_0(kr_{22})-j_2(kr_{22})]-Mh_{2C}^2/(2I_3)j_2(kr_{22})\}\ . \quad (19c)$$

In Eqs. (19a)–(19c) $I^{-1}=I_1^{-1}+I_3^{-1}$ and $I'^{-1}=I_2^{-1}+I_3^{-1}$ are combinations of the principal momenta of inertia of the molecule, I_1, I_2, and I_3.

The theoretical analysis presented here naturally leads to the possible existence of two eigenmodes. The general k dependence of the eigenfrequencies of the two modes is obtained by finding the roots of the secular equation (17), which requires only the knowledge of static quantities, namely the partial structure factors and the $d_{\alpha\beta}$ which are expressed in terms of geometrical parameters of the molecule. Before studying the $\omega(k)$ relation in the k region where the $S_{\alpha\beta}(k)$ are known, it is important to label the two solutions by recognition of their $k\rightarrow 0$ limit.

B. Solutions of the secular equation in the $k\rightarrow 0$ limit

In the $k\rightarrow 0$ limit the coefficients of the secular equation (17), reported in Eqs. (18a)–(18c), can be written as

$$a(k\rightarrow 0)=S(0)S''(0)k^2/2\ , \quad (20a)$$

$$b(k\rightarrow 0)=k_BT/(3I)h_{12}^2S(0)k^2\ , \quad (20b)$$

$$c(k\rightarrow 0)=(k_BT)^2/(3IM)h_{12}^2k^4\ , \quad (20c)$$

where, since at $k=0$ all the partial structure factors coincide,[15] we have defined

$$S(0)=S_{11}(0)=S_{22}(0)=S_{12}(0) \quad (21a)$$

in Eq. (20a):

$$S''(0)=S_{11}''(0)+S_{22}''(0)-2S_{12}''(0) \quad (21b)$$

being

$$S_{\alpha\beta}''(0)=\lim_{k\rightarrow 0}[d^2S_{\alpha\beta}(k)/dk^2]\ . \quad (22)$$

By substitution of Eqs. (20a)–(20c) into Eq. (17), the solutions for ω^2 are

$$\omega_{1,2}^2(k\to 0)=k_B T h_{12}^2/[3IS''(0)]\{1\pm[1-6S''(0)Ik^2/S(0)Mh^2]^{1/2}\} . \quad (23)$$

Therefore in this limit one of the two eigenfrequencies of the system is

$$\omega_1^2(k\to 0)=k_B T/[MS(0)]k^2 , \quad (24)$$

i.e., the ordinary sound mode with propagation velocity $v=[k_B T/MS(0)]^{1/2}$ (isothermal sound velocity), consistent with the fact that we have neglected the energy fluctuations in our analysis.

The second solution is

$$\omega_2^2(k\to 0)=2k_B T h_{12}^2/[3IS''(0)] . \quad (25)$$

Due to the finite value of the $\omega_2(k=0)$ this mode is not associated with a conserved variable and reminds one of an "optical" mode. The k dependence of its contribution to the oxygen and hydrogen density correlation functions will confirm these preliminary observations and will be discussed in the following section.

III. COMPUTER SIMULATION RESULTS

A. Dispersion curves and intensities of the two eigenmodes

In order to obtain the general k dependence of the eigenfrequencies of the two modes we have evaluated the partial structure factors $S_{\alpha\beta}(k)$ by performing a computer simulation of liquid water at $T=310$ K and $\rho=1.0$ g/cm^3. The adopted potential model (TIP4P) has been implemented by Jorgensen *et al.*[16] and consists of a Lennard-Jones interaction between the oxygen atoms (with Lennard-Jones potential parameters $\sigma=3.154$ Å and $\varepsilon=1.077\times10^{-14}$ erg), plus Coulomb interactions between two positive charges ($q=0.52e$) sitting on the hydrogen atoms and a negative one ($q=-1.04e$) on the site P indicated in Fig. 1. As is well known the TIP4P model gives a realistic description of most thermodynamical, structural and spectroscopic properties of liquid water in a wide range of temperature and pressure.[17] The molecular dynamics (MD) simulation is carried out with a standard program which makes use of generalized coordinates[18] (quaternions) and accounts for the long-range coulombic interactions through the Ewald summation method. In order to perform long runs which assure a higher statistical accuracy we have chosen to use a system of 108 molecules, which turns out to be confined in a cubic box of length $L=14.78$ Å at the chosen thermodynamic point. The integration time step is $\delta t=1.0\times10^{-15}$ s, which guarantees a satisfactory conservation of the total energy. The partial structure factors have been obtained by performing an average over five runs of 40 000 time steps of the quantities

$$S_{\alpha\beta}(k)=\langle\rho_k^{(\alpha)}(0)\rho_{-k}^{(\beta)}(0)\rangle . \quad (26)$$

The wave vector $\mathbf{k}$ is chosen to be of the form $k\equiv 2\pi(n,m,l)/L$ with $n,m,l=0,1,\ldots,10$ and the average over the independent components with the same $|k|$ is finally performed; the minimum accessible wave vector is $k_{\min}=0.4251$ Å^{-1}. The results for $S_{11}(k)$, $S_{22}(k)$, and $S_{12}(k)$ are reported in Fig. 2, for selected wave vectors. They turn out to be in good agreement with those obtained in previous MD runs by Fourier transforming the corresponding pair distribution functions calculated over 10 000 time steps with a system of $N=256$ molecules at the same state point, and used for the evaluation of the dispersion curves in Ref. 13. We wish to point out, however, that in the low-k region differences appear due to the truncation and/or extrapolation of $g_{\alpha\beta}(r)$ at long distances.

A least-squares fitting of the data in Fig. 2 with a functional form

$$S_{\alpha\beta}(k)=S(0)+S''_{\alpha\beta}(0)k^2/2+S^{\mathrm{IV}}_{\alpha\beta}(0)k^4/24 , \quad (27)$$

allows the determination of $S(0)$ and $S''_{\alpha\beta}(0)$. In particular we find $S(0)=0.065\pm0.001$, which leads to a value of the adiabatic sound velocity $v_s=[\gamma k_B T/MS(0)]^{1/2}\approx 1490$ m/s, in good agreement with the experimental value.[19] The estimate of $S''_{\alpha\beta}(0)$ is much more critical, in view of the fact that the value of ω_2 at $k=0$ is deter-

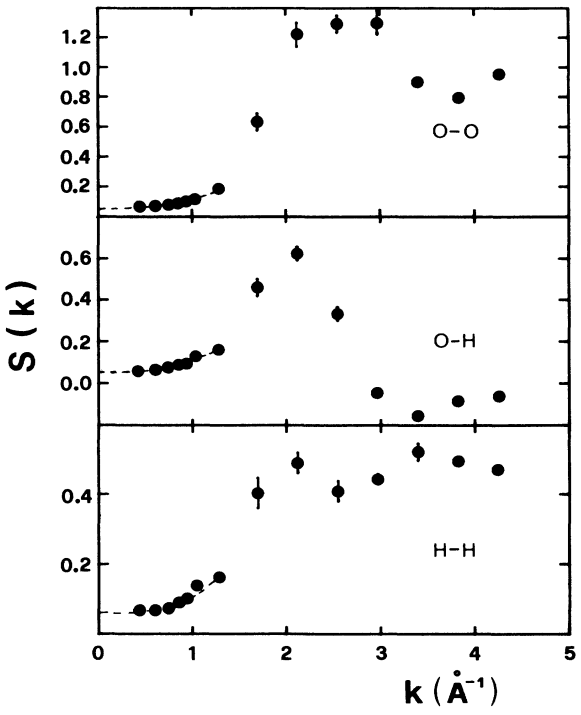

FIG. 2. The partial structure factors of water, as evaluated from Eq. (26). The error bars have been evaluated from the dispersion of the data in five independent MD runs of 40 000 time steps. The dashed lines represent the result of a fitting procedure at low k values performed following Eq. (27).

mined by the difference between close quantities [see Eq. 21(b)] and therefore the result is highly uncertain. On the other hand, to our knowledge, no relation exists between the second derivative of the partial structure factors at $k=0$ and any thermodynamic quantity, so that no check over the values obtained by the fitting procedure is possible. Even with the present more accurate results for $S_{\alpha\beta}(k)$, the uncertainty over $S''_{\alpha\beta}(0)$ leads to a value of $\omega_2(k=0)$ which is in the range $(20-300)\times 10^{12}$ s^{-1}, so that a definitive extrapolation at $k\rightarrow 0$ of the high-frequency dispersion relation is not feasible.

In Fig. 3 we report the dispersion curves for the two solutions $\omega_1(k)$ and $\omega_2(k)$ evaluated by using the $S_{\alpha\beta}(k)$ reported in Fig. 2, in the range of accessible wave vectors.

As far as the "acoustical" branch is concerned, its dispersion behavior turns out to be very close to that of a monatomic system composed of particles of mass M equal to the total mass of a water molecule and a structure factor coincident with the oxygen-oxygen one, $S_{11}(k)$. In fact the lower branch behavior is found to agree within a few % with $[k_B T/MS_{11}(k)]^{1/2}$.

The upper branch appears to be well separated from the lower one both at small and large wave vectors. This result turns out to be in contrast with our previous data reported in Ref. 13; however, we believe that the better accuracy of the present simulation data gives more reliability on the result reported here.

It is interesting to examine how the two modes contribute to the oxygen and hydrogen density correlation functions $C_{11}(k,t)$ and $C_{22}(k,t)$, that is, the diagonal elements of the correlation matrix in Eq. (3). Within the approximation used to derive Eq. (14) they read

$$C_{11}(k,t)=S_{11}(k)\{I_{11}(k)\cos[\omega_1(k)t] + I_{12}(k)\cos[\omega_2(k)t]\} , \quad (28a)$$

$$C_{22}(k,t)=S_{22}(k)\{I_{21}(k)\cos[\omega_1(k)t] + I_{22}(k)\cos[\omega_2(k)t]\} , \quad (28b)$$

where $\omega_1(k)$ and $\omega_2(k)$ are the roots of the secular equation (17) and the "amplitudes" $I_{\alpha\beta}(k)$ can be found from Eq. (14) by inserting the solutions $z=i\omega_1(k)$ and $z=i\omega_2(k)$. Details of this calculation are reported in Appendix B. By definition,

$$I_{11}(k)+I_{12}(k)=I_{21}(k)+I_{22}(k)=1 , \quad (29)$$

and the k dependence of $I_{11}(k)$ and $I_{22}(k)$ is reported in Fig. 4. The relevant physical features of their behavior, already stressed in Ref. 13, are the following. At $k=0$ $I_{11}(0)=I_{21}(0)=1$ [and consequently $I_{12}(0)=I_{22}(0)=0$], which points out that only the "acoustic" mode contributes to the oxygen and hydrogen density fluctuations. This result is consistent with the fact that, in exploring the behavior of the system at long wavelengths, the position of the reference point over the molecule used to account essentially for the numerical density fluctuations becomes irrelevant. At increasing k, $I_{11}(k)$ remains very close to 1, whereas $I_{22}(k)$ increases and reaches 1 at $k\approx 3$

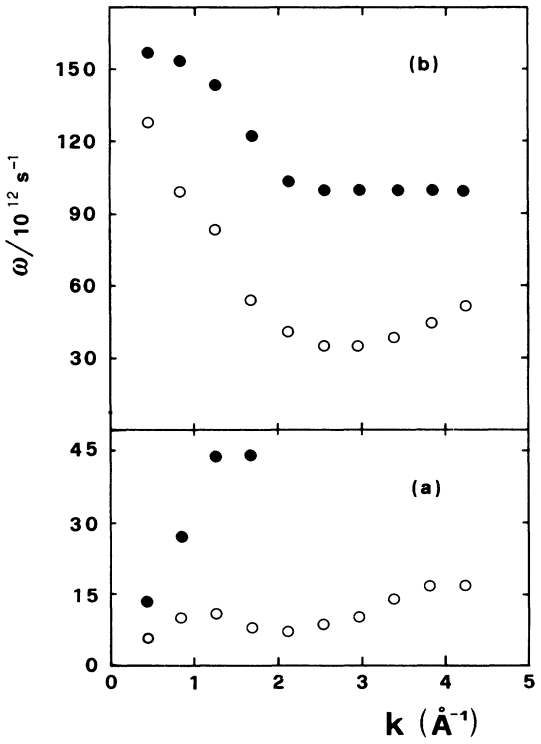

FIG. 3. The dispersion relation of the (a) low and (b) high energy modes of water as evaluated solving the secular equation (17) (open circles) and from the peak positions in $\omega^2 S(k,\omega)$ (solid circles).

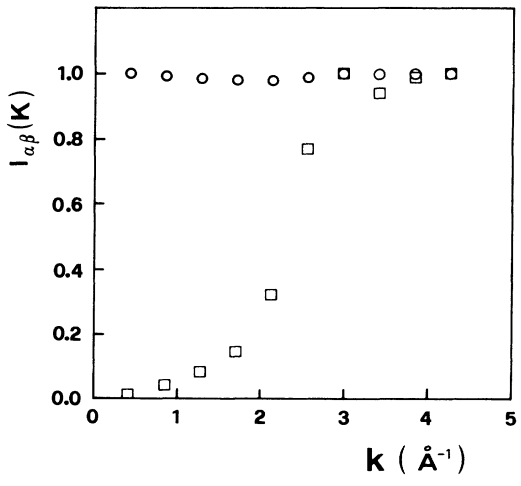

FIG. 4. The "amplitude" $I_{11}(k)$ of the low-frequency mode in the oxygen density correlation function defined in Eq. (28a) (circles), and that of the high-frequency mode in the hydrogen density correlation function $I_{22}(k)$ in Eq. (28b) (squares), as a function of the wave vector.

$Å^{-1}$. This result points out that the oxygen density fluctuations are governed only by the lower-frequency mode, whereas the hydrogen ones are progressively dominated by the higher-frequency solution.

On the basis of these observations, some conclusions can be drawn which clarify the nature of the high-frequency mode. Namely, (a) the k dependence of $\omega_2(k)$, which shows a marked dispersion, points out the collective character of this mode; (b) three different results give a clear evidence that the rotational degrees of freedom are involved in the dynamics of this collective mode, i.e., (i) $\omega_2(k \to 0)$ has a finite value, (ii) this value depends on the momenta of inertia of the molecule, and (iii) only the hydrogen density fluctuations are affected by this high-frequency mode.

B. The density-density correlation functions

In order to have a direct check of the reliability of our analysis in terms of the two-component dynamical variable of Eq. (1), we have evaluated the correlation function matrix in Eq. (3), making use of the configurations generated by the MD simulation. The correlation functions have been sampled with a time interval $\Delta t = 10^{-14}$ s and evaluated up to $T \approx 2 \times 10^{-11}$ s, for $k = 2n\pi/L$ ($n = 1, \ldots, 10$). The results are reported in terms of normalized density autocorrelation functions

$$F_{\alpha\beta}(k,t) = C_{\alpha\beta}(k,t)/S_{\alpha\beta}(k) \ . \tag{30}$$

The $F_{11}(k,t)$ are reported in Fig. 5; we note the well-known de Gennes slowing-down effect[20] at wave vectors corresponding to the maximum of $S_{11}(k)$, namely $n \approx 4$, followed by a decrease of the decay time approaching the free-particle regime at highest n values. The hydrogen density autocorrelation functions $F_{22}(k,t)$ are found to present the same overall behavior as $F_{11}(k,t)$, any remarkable difference being restricted in the short-time region. The comparison between $F_{11}(k,t)$ and $F_{22}(k,t)$, at the investigated k values and in the time range $0 < t < 0.2$ ps is shown in Fig. 6. One can note that $F_{22}(k,t)$ has a faster initial decay, which becomes progressively much more pronounced at increasing wave vectors.

By Eq. (A11a) the second derivative of $F_{11}(k,t)$ at $t = 0$ can be written as

$$F''_{11}(k,t=0) = k_B T/[M S_{11}(k)][1 + M R_{1C}^2/(3I)]k^2 \tag{31}$$

which indicates that, with respect to the center-of-mass value, a correction is present which accounts for the rotational degrees of freedom contribution to the dynamics of the oxygen atoms. It is worth noticing that this correction turns out to be independent of k and quite small in the specific case of a water molecule, amounting only to $\approx 5\%$ of the total. The result for the second derivative of $F_{22}(k,t)$ [see Eq. (A11c)] can explain on a quantitative basis its short-time behavior. Indeed in this case the rotational correction turns out to be much greater and moreover k dependent. In the two extreme cases of $k \to 0$ and $k \to \infty$ one obtains

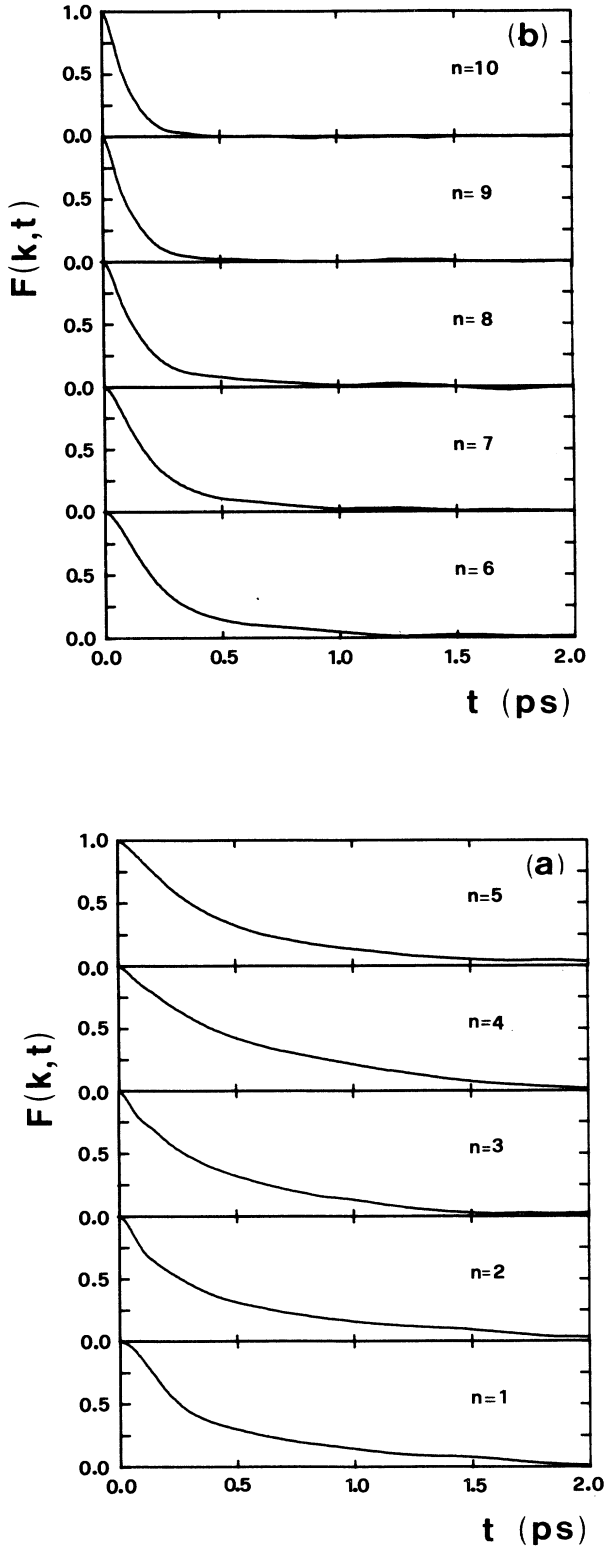

FIG. 5. MD-calculated intermediate scattering function of the oxygen atoms, for $k = 2\pi n/L$ ($n = 1,2, \ldots, 10$).

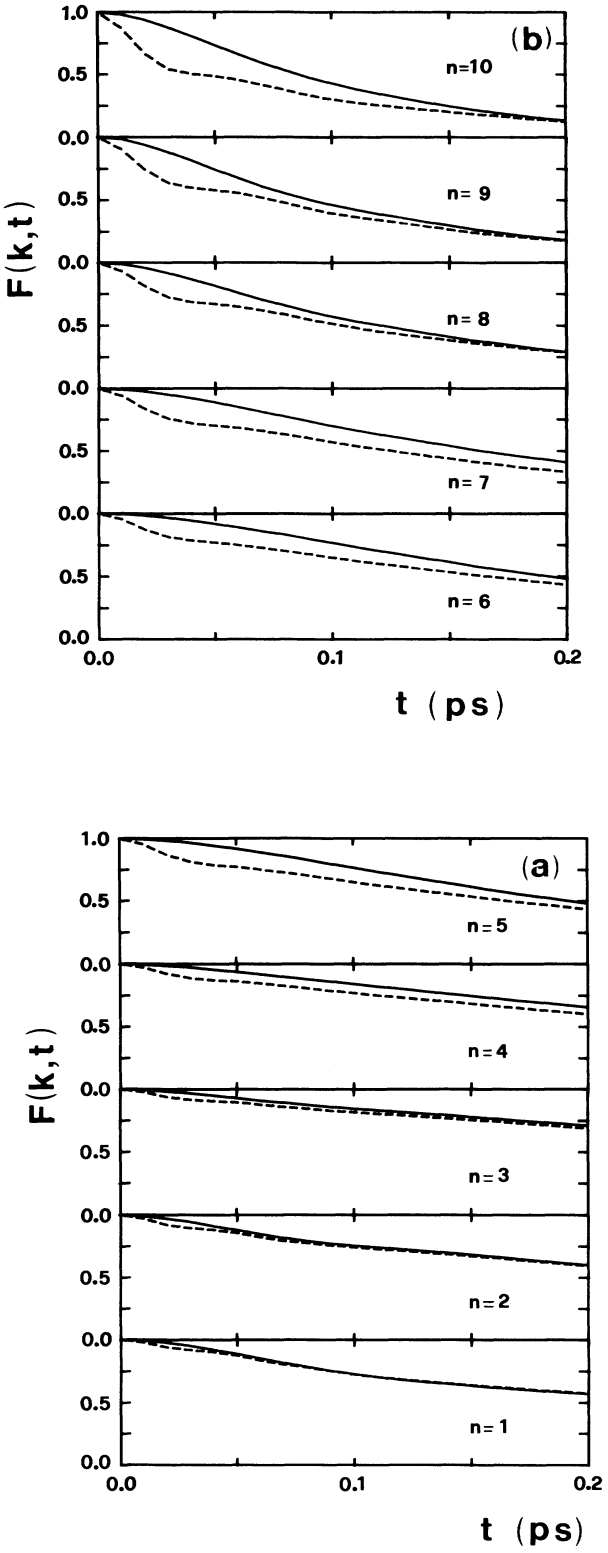

FIG. 6. MD-calculated intermediate scattering function of the oxygen and hydrogen atoms (solid and dashed lines, respectively), for $k=2\pi n/L$ ($n=1,2,\ldots,10$).

$$F''_{22}(k\to 0,t=0)=k_BT/[MS_{22}(k)][1+Mh_{2C}^2/(3I)]k^2\ , \tag{32a}$$

$$F''_{22}(k\to\infty,t=0) =k_BT/[2MS_{22}(k)]\{1+[h_{2C}^2/I_1+r_{22}^2/(4I_2) +(h_{2C}^2+r_{22}^2/4)/I_3]M/3\}k^2\ , \tag{32b}$$

which in the case of the water molecule leads to corrections of 3.6 and 8.6 at $k\to 0$ and $k\to\infty$, respectively. These results about the time dependence of the correlation functions and the following discussion on the relative spectra show that the interpretation of the experimental neutron scattering data, in terms of the center-of-mass density fluctuations, can be misleading for molecular systems. However, since both the intermediate scattering functions are found to decay to zero on the same time scale, the low-frequency region of their spectra is expected to be virtually the same, any remarkable difference being confined at high frequency.

The oxygen density correlation function can reasonably be compared with previous computer simulation results for the center-of-mass density correlation function reported by Rahman and Stillinger[10] and Wojcik and Clementi,[12] who used different potential models, namely the so called ST2 (Ref. 10) and MCY, respectively, in the molecular simulation of liquid water. It is worth noticing that our data are in reasonable agreement with those of Rahman and Stillinger:[10] the different decay time of the intermediate scattering functions is interpretable in terms of the lower temperature of their simulation. On the contrary a marked discrepancy is found between our results and those of Wojcik and Clementi,[12] whose simulation is at the same thermodynamic point of the present investigation. At small wave vectors their intermediate scattering functions show a pronounced oscillatory behavior which is absent in our results (see Fig. 5). These differences point out how the dynamical properties are more sensitive to the potential model than the static ones.

Let us show now to what extent the proposed theoretical analysis is able to predict the computer simulation results and moreover discuss the differences between the oxygen and hydrogen density fluctuation spectra. As is usually done,[3] we report the peaks of the longitudinal current density spectrum, i.e., $\omega^2S(k,\omega)$ as a measure of the dispersion relation, even if we are aware of the fact that it gives a stringent test only in the presence of well-defined frequency modes. The longitudinal current density spectra are presented in Figs. 7 and 8, for oxygen and hydrogen, respectively. The resultant peak frequencies are shown in Fig. 3: we note that the high-frequency peaks appear only in the hydrogen spectrum and its $\omega(k)$ dependence is in qualitative agreement with the theoretical predictions, whereas the low acoustic peaks, which are present in both spectra, have a frequency substantially higher than the values calculated by the theoretical model and are found to be in good agreement both with computer simulation results of Wojcik and Clementi,[12] as

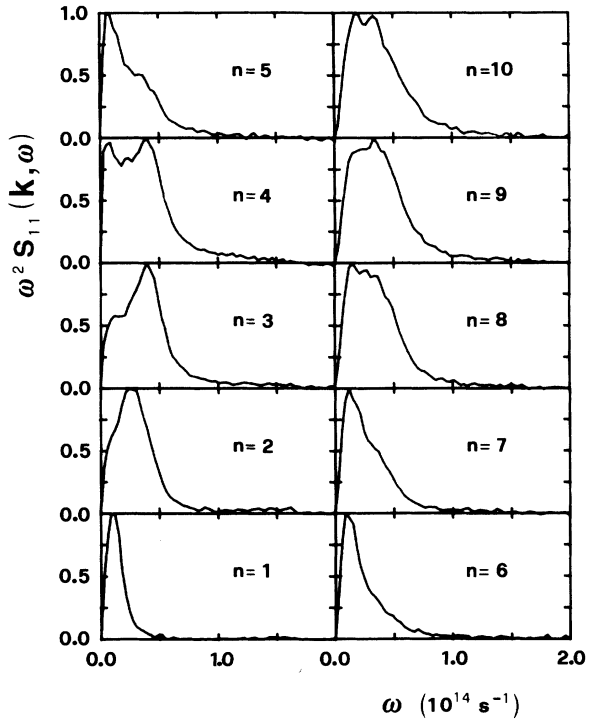

FIG. 7. MD results for $\omega^2 S_{11}(k,\omega)$ as a function of ω at the investigated k values, in arbitrary units.

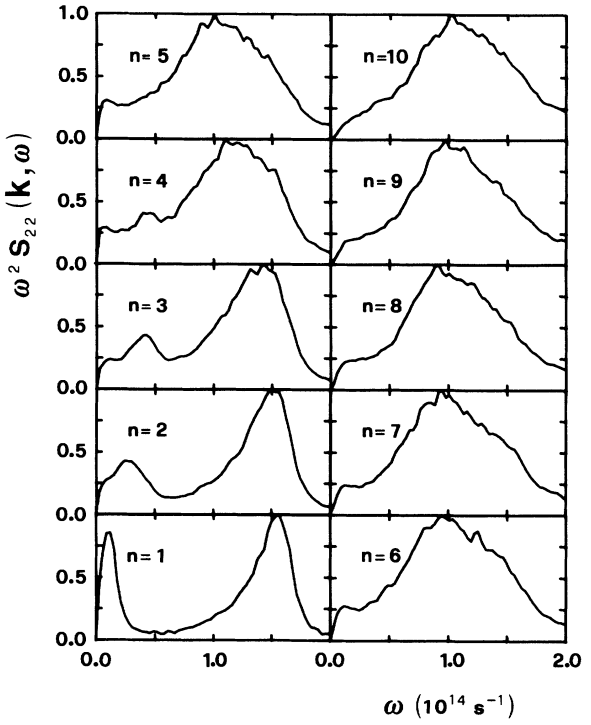

FIG. 8. MD results for $\omega^2 S_{22}(k,\omega)$ as a function of ω at the investigated k values, in arbitrary units.

well as with the experimental data of Teixeira *et al.*[9]

As already stressed, the k dispersion of the high-frequency mode $\omega_2(k)$, derived both from the theoretical analysis and the computer simulation results, points out the collective character of this mode. To confirm this conclusion we have separately evaluated the single-particle contribution to the hydrogen density correlation function, i.e.,

$$F_{22}^{(s)}(k,t)=\frac{1}{N}\sum_i \langle \{\exp[i\mathbf{k}\cdot\mathbf{r}_i^{(H(1))}(0)]+\exp[i\mathbf{k}\cdot\mathbf{r}_i^{(H(2))}(0)]\}\{\exp[i\mathbf{k}\cdot\mathbf{r}_i^{(H(1))}(t)]+\exp[i\mathbf{k}\cdot\mathbf{r}_i^{(H(2))}(t)]\}\rangle \ . \tag{33}$$

The corresponding $\omega^2 S_{22}^{(s)}(k,\omega)$, where $S_{22}^{(s)}(k,\omega)$ represents the Fourier transform of $F_{22}^{(s)}(k,t)$, show a broad band centered at a frequency $\omega_M \approx 100\times 10^{12}$ s^{-1}, which remains unchanged at increasing wave vector. At small wave vectors $F_{22}(k,t)$ and $F_{22}^{(s)}(k,t)$ are markedly different, whereas, as expected, at large k values they become closer and closer. In fact we note that ω_M almost coincides with the values of $\omega_2(k)$ at high wave vectors (see Fig. 3). Moreover the general behavior of the $\omega^2 S_{22}(k,\omega)$ and $\omega^2 S_{22}^{(s)}(k,\omega)$ is the same in this k region. Examples of these spectra are reported in Fig. 9. In the same figure we present also the quantity

$$\rho_{22}(\omega)=\sum_{k=1}^{10} k^2 S_{22}(k,\omega) \ , \tag{34}$$

which is a rough estimate of the hydrogen projected density of states: its shape is found to be in good agreement with that of $S_{22}^{(s)}(k,\omega)$, in the high-frequency region. As expected at low frequencies the two functions are different, because the diffusive motions appear only in the self-contribution to the dynamic structure factor.

These results unambiguously point out that in the small-k region the hydrogen density fluctuations are governed by collective excitations and not by the single-molecule motion which instead, as is well known, is the relevant one in the dynamics of these fluctuations at large wave vectors.

IV. DISCUSSION AND CONCLUSIONS

Our theoretical analysis and MD study of the density fluctuations in water stresses the following general results:

(i) The analysis of the experimental data in terms of center-of-mass-density fluctuations, overlooking the orientational dynamics of the molecules, can lead to incorrect conclusions for molecular fluids.

(ii) When the orientational dynamics is taken into account, for example, through the density fluctuations of

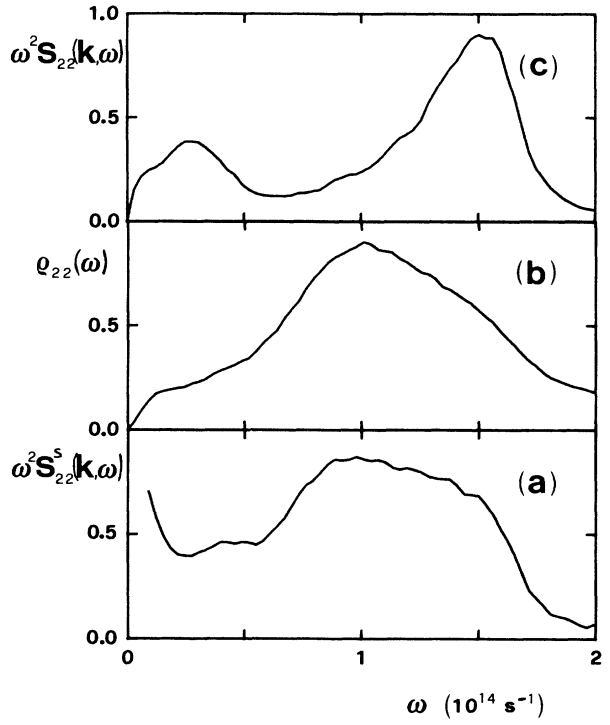

FIG. 9. (a) $\omega^2 S^{(s)}_{22}(k,\omega)$ vs ω at $k=0.85$ Å^{-1} as evaluated from the MD trajectories. (b) $\rho_{22}(\omega)$ defined in Eq. (34). (c) $\omega^2 S_{22}(k,\omega)$ vs ω at $k=0.85$ Å^{-1}. The intensity units are arbitrary.

the individual atomic species, both MD simulations and a first-order memory function approach predict the presence of two collective excitations in the liquid, at wavelengths comparable with the intermolecular distances.

(iii) The ω-vs-k dispersion relation for these excitations, as evaluated from the peak positions of $\omega^2 S_{\alpha\beta}(k,\omega)$ obtained by computer simulation, are only in qualitative agreement with the predictions of the theoretical model. As a matter of fact this discrepancy is evidence of the well-known limit of the second-moment approximation already emphasized in the case of liquid argon,[21] and stresses the relevance of the MD simulation for an unambiguous comparison with the experimental data.

Let us now separately discuss the physical origin of the low- and high-frequency modes, on the basis of the comparison with the experimental findings.

A. Low-frequency mode

A collective excitation at frequencies well above those expected by extrapolating from the hydrodynamic limit, as found in the present investigation, has already been observed in a coherent neutron scattering experiment on D_2O by Teixeira *et al.*[9] and widely investigated by a recent MD simulation of MCY water by Wojcik and Clementi.[12] The observed dispersion relation can in principle originate either from a positive dispersion of the ordinary sound waves at finite wave vectors, or from the propagation of an additional "fast sound" mode, quite peculiar of liquid water. Under the latter hypothesis two peaks should appear in the low-frequency region of the density fluctuation spectra: although the frequency resolution of our simulation is high enough[22] to allow the detection of both peaks, unless highly broadened, only one peak appears in the explored k region. This peak is common to both the hydrogen and oxygen dynamical structure factors and can therefore be associated with a translational excitation. By comparison with the theoretical results, this mode can be identified with the ordinary sound mode, which shows a linear dispersion relation with velocity $v_s=1490$ m/s in the hydrodynamic regime.

Although the above arguments against the interpretation of the experimental data in terms of "fast" sound could not appear very strong, much evidence can be put forward in favor of the interpretation in terms of a positive sound dispersion.

Indeed an anomalous positive sound dispersion has already been observed in monoatomic fluids,[1] and it can also be argued, as suggested in Ref. 12, that the attractive part of the interaction potential plays some role in determining the relevance of this anomalous behavior. From this point of view it is not surprising that in water the anomalous sound dispersion is particularly enhanced, owing to the presence and cooperativity of the hydrogen bond interaction. Moreover, in other hydrogen-bonded liquids, such as water-alcohol mixtures, a positive dispersion larger than that found in "simple" liquids has already been observed.[23]

Two possible mechanisms can be envisaged as the origin of the anomalous sound dispersion in water. The first one is dynamical in character and lies on the existence of a relaxing variable which couples with the density fluctuations, thus inducing a relaxation in the frequency-dependent transport coefficients of the fluid and a consequent decrease of the sound absorption. This argument was excluded by Teixeira *et al.*[9] since the dielectric relaxation time corresponds to frequencies typical of the light scattering experiments and therefore one would expect a variation of the sound velocity in the frequency range explored by the Brillouin scattering. On the contrary both ultrasonic and light scattering measurements, in the whole k range explored, give the same value of the sound velocity.

However, we want to note that other relaxation mechanisms can be invoked. In particular low frequency depolarized Raman spectra of water show evidence for a relaxation mechanism with characteristic time τ_{Raman}, of the order of a few picoseconds,[24] corresponding to a frequency much greater than that of the Brillouin doublet, but still lower than those investigated by neutron scattering and MD simulation. A recent MD simulation of the low-frequency Raman spectra[25] has identified the dynamical variables which generate this spectral contribution to be mainly the relative displacements of the molecules. One can reasonably expect that these dynamical variables couple strongly to the density fluctuations at high k values. At $T=30$ °C, being $\tau_{\text{Raman}}\approx 5\times 10^{-13}$ s, the positive sound dispersion would take place at k of the order of $(v_s\tau_{\text{Raman}})^{-1}\approx 10^{-1}$ Å^{-1}.

Another possible contribution to the positive sound dispersion can be found in the peculiar shape of the static structure factor of water at very long wavelengths. Indeed small-angle x-ray diffraction[26,27] indicate that even at room temperature the measured $S(k)$ shows a negative derivative up to k values (say k^*) of the order of at least a few hundredths of Å^{-1}. In this case a simple first-order memory function theory which predicts

$$v_s(k)=\{\gamma k_B T/[MS(k)]\}^{1/2} \tag{35}$$

can qualitatively suggest an increase of the sound velocity at wave vectors intermediate between those probed by light scattering and neutron measurements. In this picture the density fluctuations with wavelength larger than $\Lambda=2\pi/k^*$ see the fluid as a continuum and propagate with the ordinary sound velocity. On the contrary the fluctuations with wavelengths lower than Λ propagate inside the icelike structures which generate the anomaly in the structure factor, following a dispersion law similar to that of the longitudinal acoustic phonons in hexagonal ice (Ih).[28] These icelike structures are nothing but the "strong bonded patches of water molecules" invoked by Teixeira *et al.* in order to explain both the anomaly of the static structure factor[26] and the coherent neutron scattering data.[9]

Assuming that the above described mechanisms are the correct ones to explain the observed sound dispersion, one can also envisage the reason why this phenomenon in water is stronger than in simple fluids. Indeed on one side anomalies at low k in the static structure factor have been found only in water and aqueous solutions; on the other hand the coupling between the relaxation mechanisms and the density fluctuations occurs at wavelengths much greater in water than in simple liquids.

In conclusion we believe that the peaks observed in both the simulated and experimental $\omega^2 S_{\alpha\beta}(k,\omega)$ are a manifestation of the ordinary sound waves which suffer a dispersion of the velocity and a decrease of the damping factor.

B. High-frequency mode

The high-frequency mode is a new feature predicted by the present theoretical analysis. It is found to propagate through the hydrogen atoms and is observed by computer simulation of the appropriate density fluctuations, reported in this paper for the first time.

The contribution of these density fluctuations to an experimental neutron scattering spectrum is nevertheless very low due to the weak intensity of this high-frequency mode. By using the computer simulation results for the partial dynamical structure factors combined with the appropriate coherent scattering length, we have reconstructed the "experimental" $S(k,\omega)$ which is reported in Fig. 10 for two particular wave vectors. As is evident the presence of this mode manifests only as an enhancement of the high-frequency part of the spectrum so small that it can hardly be observable experimentally.

Two main features allow one to conclude that the high-frequency mode has a collective character; namely, the wave-vector-dependent dispersion relation (see Fig. 3), and the comparison between the spectra of the total intermediate hydrogen scattering function $F_{22}(k,t)$ and its single-particle contribution $F_{22}^{(s)}(k,t)$.

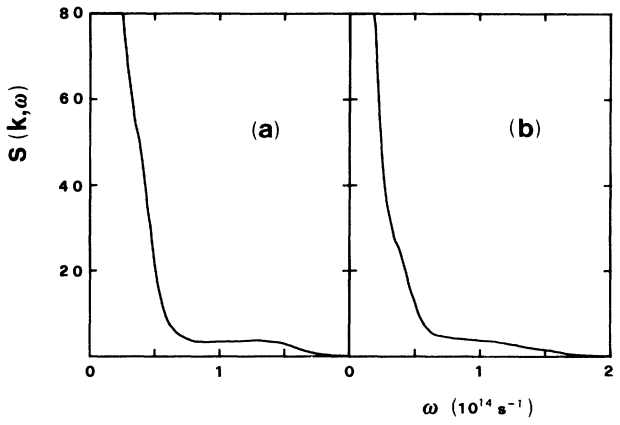

FIG. 10. The "experimental" $S(k,\omega)$ evaluated from the MD trajectories, combining the partial spectra with scattering length appropriate for a D_2O molecule, i.e., $S(k,\omega)=7.63S_{11}(k,\omega)+2.11S_{22}(k,\omega)+8.03S_{12}(k,\omega)$. (a) $k\approx 1.28$ Å^{-1}; (b) $k\approx 1.7$ Å^{-1}; the intensity units are arbitrary.

The rotational degrees of freedom are unambiguously involved in the dynamics of this mode, in view of the fact that its eigenfrequency is dependent upon the momenta of inertia of the molecule and only the dynamics of the hydrogen atoms is affected by this mode. As a final remark we note that the frequency values of the mode (in the small- and high-wavevector regions) appear to be in the range proper to the librational motions of the molecule, i.e., 10^{14} Hz.

ACKNOWLEDGMENTS

The authors wish to thank Dr. U. Balucani, Professor S. W. Lovesey, Professor V. Mazzacurati and Professor M. Nardone for stimulating discussions. The computing time was made available under convention between CNR (Consiglio Nazionale delle Ricerche) and CINECA (Centro di calcolo elettronico interuniversitario dell'Italia nord-orientale).

APPENDIX A

In this appendix we report a detailed evaluation of the matrix elements of $\underline{M}(k,t=0)$, as defined in Eq. (16). Let us start from the calculation of

$$\langle \dot{\rho}_k(0)\cdot\dot{\rho}_k^{\dagger}(0)\rangle \ , \tag{A1}$$

where from the definitions (4), 5(a), and 5(b)

$$\dot{\rho}_k(0)=\begin{bmatrix}\dot{\rho}_k^{(1)}(0)\\ \dot{\rho}_k^{(2)}(0)\end{bmatrix} , \tag{A2}$$

with

$$\dot{\rho}_k^{(1)}(0)=(1/N^{1/2})\sum_i (i\mathbf{k}\cdot\dot{\mathbf{r}}_i^{(0)})\exp[i\mathbf{k}\cdot\mathbf{r}_i^{(0)}(0)] , \tag{A3a}$$

$$\dot{\rho}_k^{(2)}(0)=(1/N^{1/2})\sum_i(\{i\mathbf{k}\cdot\dot{\mathbf{r}}_i^{(\mathrm{H}(1))}\exp[i\mathbf{k}\cdot\mathbf{r}_i^{(\mathrm{H}(1))}(0)] + (i\mathbf{k}\cdot\dot{\mathbf{r}}_i^{(\mathrm{H}(2))})\exp[i\mathbf{k}\cdot\mathbf{r}_i^{(\mathrm{H}(2))}(0)]\}) . \tag{A3b}$$

Having assumed the molecule to be a rigid body one has

$$\dot{\mathbf{r}}_i^{(\alpha)}=\dot{\mathbf{r}}_i^{(C)}+\boldsymbol{\omega}_i\times\mathbf{r}_i^{(C\alpha)} \tag{A4}$$

where α stands for 0, H(1), or H(2); $\dot{\mathbf{r}}_i^{(C)}$ is the velocity of the center of mass of molecule i, ω_i its angular velocity and $\mathbf{r}_i^{(C\alpha)}$ represents the vector joining the center of mass and the point α over the molecule.

The Hamiltonian of the system can be written as

$$\mathcal{H}=\sum_i M(\dot{r}_i^{(C)})^2/2+\sum_i \underline{T}_i\cdot\boldsymbol{\omega}_i\cdot\boldsymbol{\omega}_i/2+V(r_i^{(C)},\Omega_i) \tag{A5}$$

M being the total mass of the molecule, $\underline{T}_i$ the inertia tensor referred to a laboratory fixed frame, and $V(r_i^{(C)},\Omega_i)$ the total potential energy. In general the evaluation of the matrix element of (A1) requires one to perform the ensemble average of

$$\langle\dot{\rho}_k^{(\alpha)}\dot{\rho}_{-k}^{(\beta)}\rangle=\langle(1/N^{1/2})\sum_i[i\mathbf{k}\cdot(\dot{\mathbf{r}}_i^{(C)}+\boldsymbol{\omega}_i\times\mathbf{r}_i^{(C\alpha)})\exp(i\mathbf{k}\cdot\mathbf{r}_i^{(\alpha)})](1/N^{1/2})\sum_j[-i\mathbf{k}\cdot(\dot{\mathbf{r}}_j^{(C)}+\boldsymbol{\omega}_j\times\mathbf{r}_j^{(C\beta)})\exp(i\mathbf{k}\cdot\mathbf{r}_j^{(\beta)})]\rangle \tag{A6}$$

The Hamiltonian being a quadratic form in $\dot{r}_i^{(C)}$ and ω_i, all the terms of Eq. (A6) in which $i\neq j$ vanish because they contain either $\langle\dot{r}_i^{(C)}\rangle$ or $\langle\omega_i\rangle$ which can be assumed to be zero. For the same reason $\langle\dot{\boldsymbol{\rho}}_k^{(\alpha)}\cdot\boldsymbol{\rho}_{-k}^{(\beta)}\rangle=0$, which proves that the matrix $\underline{\Omega}(k)$, which appears in Eq. (8), is identically zero. Therefore Eq. (A6) turns out to be the sum of N identical terms, each one being the average of a single molecule quantity, and can be written as

$$\langle\dot{\boldsymbol{\rho}}_k^{(\alpha)}\cdot\dot{\boldsymbol{\rho}}_{-k}^{(\beta)}\rangle=\langle[i\mathbf{k}\cdot(\dot{\mathbf{r}}_1^{(C)}+\boldsymbol{\omega}_1\times\mathbf{r}_1^{(C\alpha)})]\exp(i\mathbf{k}\cdot\mathbf{r}_1^{(\alpha)})[-i\mathbf{k}\cdot(\dot{\mathbf{r}}_1^{(C)}+\boldsymbol{\omega}_1\times\mathbf{r}_1^{(C\beta)})]\exp(i\mathbf{k}\cdot\mathbf{r}_1^{(\beta)})\rangle . \tag{A6a}$$

The average is then more easily performed in a molecular reference frame with the axes coincident with the inertial principal ones, in which the tensor $\underline{T}$ is diagonal; in such a reference frame (which is specified in Fig. 1), the rotational kinetic energy reads

$$K_R=[I_1\omega_1^2+I_2\omega_2^2+I_3\omega_3^2]^{1/2} . \tag{A7}$$

Out of the four terms present in equation (A6a) only two survive, being

$$\langle(i\mathbf{k}\cdot\dot{\mathbf{r}}_1^{(C)})\exp(i\mathbf{k}\cdot\mathbf{r}_1^{(\alpha)})[-i\mathbf{k}\cdot(\boldsymbol{\omega}_1\times\mathbf{r}_1^{(C\beta)})]\exp(-i\mathbf{k}\cdot\mathbf{r}_1^{(\beta)})\rangle=\langle i\mathbf{k}\cdot\dot{\mathbf{r}}_1^{(C)}\exp(i\mathbf{k}\cdot\mathbf{r}_1^{(\alpha)})\rangle\langle-i\mathbf{k}\cdot(\boldsymbol{\omega}_1\times\mathbf{r}_1^{(C\beta)})\exp(i\mathbf{k}\cdot\mathbf{r}_1^{(\beta)})\rangle=0 . \tag{A8}$$

One is left with the calculation of the quantities

$$\langle(\mathbf{k}\cdot\dot{\mathbf{r}}_1^{(C)})^2\exp[i\mathbf{k}\cdot(\mathbf{r}_1^{(C\alpha)}-\mathbf{r}_1^{(C\beta)})]\rangle , \tag{A9a}$$

$$\langle[\mathbf{k}\cdot(\boldsymbol{\omega}_1\times\mathbf{r}_1^{(C\alpha)})][\mathbf{k}\cdot(\boldsymbol{\omega}_1\times\mathbf{r}_1^{(C\beta)})\exp[i\mathbf{k}\cdot(\mathbf{r}_1^{(C\alpha)}-\mathbf{r}_1^{(C\beta)})]\rangle , \tag{A9b}$$

which involve an average over the distribution of center of mass and angular velocity as well as an angular average over the possible orientation of the molecule. The latter is accomplished after having expressed the exponential in a Rayleigh expansion,

$$\exp[i\mathbf{k}\cdot(\mathbf{r}_1^{(C\alpha)}-\mathbf{r}_1^{(C\beta)})]=4\pi\sum_{l,m}(i)^l j_l(k|\mathbf{r}_1^{(C\alpha)}-\mathbf{r}_1^{(C\beta)}|)Y_{lm}(\Omega_k)Y_{lm}^*(\Omega_r) , \tag{A10}$$

in which $j_l(x)$ is the lth spherical Bessel function and $Y_{lm}(\Omega)$ are the normalized spherical harmonics, whose argument is the direction cosine either of $\mathbf{k}$ or $\mathbf{r}_1^{(C\alpha)}-\mathbf{r}_1^{(C\beta)}$. By writing the dot products in Eq. (A9b) in terms of spherical harmonics (of argument Ω_k) and finally observing that only those terms which contain ω_α^2 will survive, all the contributions to the matrix elements of Eq. (A1) can be evaluated. The result is

$$\langle\dot{\rho}_k^{(1)}\dot{\rho}_{-k}^{(1)}\rangle=[k_BT/M+(1/I_1+1/I_3)k_BTR_{1C}^2/3]k^2 , \tag{A11a}$$

$$\langle\dot{\rho}_k^{(1)}\dot{\rho}_{-k}^{(2)}\rangle=\langle\dot{\rho}_k^{(2)}\dot{\rho}_{-k}^{(1)}\rangle=2\{k_BT/Mj_0(kr_{12})-k_BT/3(1/I_1+1/I_3)R_{1C}h_{2C}[j_0(kr_{12})+j_2(kr_{12})] - k_BT/I_3(2h_{2C}/R_{1C}+1)R_{1C}^2\sin^2\chi j_2(kr_{12})\}k^2 , \tag{A11b}$$

$$\langle\dot{\rho}_k^{(2)}\dot{\rho}_{-k}^{(2)}\rangle=2(k_BT/M[1+j_0(kr_{22})]+k_BT/3\{h_{2C}^2/I_1+(r_{22}/2)^2/I_2+[h_{2C}^2+(r_{22}/2)]/I_3\} - k_BT/I_3h_{2C}^2j_2(kr_{22})+k_BT/(3I_3)[h_{2C}^2-(r_{22}/2)^2][j_0(kr_{22})+j_2(kr_{22})] - k_BT/(3I_2)(r_{22}/2)^2[j_0(kr_{22})+j_2(kr_{22})]+k_BT/(3I_1)h_{2C}^2[j_0(kr_{22})+j_2(kr_{22})])k^2 . \tag{A11c}$$

The definition of all the symbols can be found in Fig. (1). Equations (A11a)–(A11c) illustrate the differences in the second moment of the oxygen and hydrogen density correlation functions. For the molecular center of mass one would obtain

$$\langle \dot{\rho}_k^{(C)} \dot{\rho}_{-k}^{(C)} \rangle = (k_B T/M)k^2 \ . \tag{A12}$$

The correction to this result for the oxygen second moment (Eq. (A11a) turns out to be quite simple and small in the case of a water molecule in view of the fact that $R_{1C} \approx 0$, but more involved (and wave-vector dependent) for the other two moments [see Eqs. (A11b) and (A11c). The results (A11a)–(A11c) along with Eq. (16) allow the evaluation of the coefficients of the secular equation (15), reported in Eqs. (18a)–(18c).

APPENDIX B

In this appendix we report the details of the calculation of the oxygen-oxygen density correlation function, evaluated under the assumption that the damping of the two contributing modes can be neglected. We derive the expression for the amplitudes of the two modes whose frequencies are found by solving the secular Eq. (15). We start from Eq. (14) which can be written as

$$\hat{\underline{C}}(k,z) = z[z^2 \underline{I} + \underline{M}(k,0)]^{-1} \underline{C}(k,0) \ , \tag{B1}$$

where the matrices $\underline{M}(k,0)$ and $\underline{C}(k,0)$ are defined in Eqs. (16) and (6), respectively. The solution for the Laplace transform of the oxygen density correlation function $\hat{C}_{11}(k,z)$ can be written as

$$\hat{C}_{11}(k,z) = z[C_{11}(0)z^2 + C_{11}(0)M_{22}(0) - C_{12}(0)M_{12}(0)]/[(z^2 - z_1^2)(z^2 - z_2^2)] \ , \tag{B2}$$

where z_1 and z_2 are the solutions of the secular equation and $z = i\omega$. Equation (B2) can be easily split into the sum of two terms, namely

$$\begin{aligned} \hat{C}_{11}(k,z) = z(z_1^2 - z_2^2)^{-1}\{&[C_{11}(0)z_1^2 - C_{12}(0)M_{12}(0) + C_{11}(0)M_{22}(0)](z^2 - z_1^2)^{-1} \\ &- [C_{11}(0)z_2^2 - C_{12}(0)M_{12}(0) + C_{22}(0)M_{22}(0)](z^2 - z_2^2)^{-1}\} \ . \end{aligned} \tag{B3}$$

By inserting into Eq. (B3) the identity

$$(z^2 - z_1^2)^{-1} = [(z - z_1)^{-1} - (z + z_1)^{-1}]/(2z_1) \tag{B4}$$

and after having performed the inverse Laplace transform, one finds

$$\begin{aligned} C_{11}(k,t) = (\omega_2^2 - \omega_1^2)^{-1}\{&[-C_{11}(0)\omega_1^2 - C_{12}(0)M_{12}(0) + C_{11}(0)M_{22}(0)]\cos\omega_1 t \\ &+ [-C_{11}(0)\omega_2^2 - C_{12}(0)M_{12}(0) + C_{11}(0)M_{22}(0)]\cos\omega_2 t\} \end{aligned} \tag{B5}$$

which can be written as

$$C_{11}(k,t) = C_{11}(0)[I_{11}(k)\cos(\omega_1 t) + I_{12}(k)\cos(\omega_2 t)] \tag{B6}$$

with an obvious definition of $I_{11}(k)$ and $I_{22}(k)$. From Eq. (B5) it is immediately shown that

$$I_{11}(k) + I_{12}(k) = 1 \ . \tag{B7}$$

Similar calculations can be performed to derive the hydrogen density correlation function $C_{22}(t)$ which turns out to be

$$C_{22}(k,t) = C_{22}(0)[I_{21}(k)\cos(\omega_1 t) + I_{22}(k)\cos(\omega_2 t) \ . \tag{B8}$$

By making use of the expression for $\langle \dot{\rho}_k^{(\alpha)} \dot{\rho}_{-k}^{(\beta)} \rangle$ derived in Appendix A [see Eqs. (A11a)–(A11c)] and performing the limit of $k \to 0$ one obtains

$$I_{11}(k \to 0) = I_{21}(k \to 0) = 1 \ . \tag{B9}$$

[1]For extensive reviews see, for example, J. R. D. Copley and S. W. Lovesey, Rep. Prog. Phys. **38**, 461 (1975); K. E. Larsson, Phys. Chem. Liq. **95**, 273 (1983).

[2]L. Van Hove, Phys. Rev. **95**, 249 (1954).

[3]A. Rahman, Phys. Rev. Lett. **19**, 420 (1967); G. H. Chung and S. Yip, Phys. Lett. **50A**, 175 (1974).

[4]W. E. Alley, B. J. Alder, and S. Yip, Phys. Rev. A **27**, 3174 (1983).

[5]D. Levesque, L. Verlet, and J. Kurkijarvi, Phys. Rev. A **7**, 1690 (1973); M. Schoen, R. Vogelsang, and C. Hoheisel, Mol. Phys. **57**, 445 (1986); I. M. de Schepper, E. G. D. Cohen, C. Bruin, J. C. van Rijs, W. Montfrooij, and L. A. de Graaf, Phys. Rev. A **38**, 271 (1988).

[6]A. Rahman, Phys. Rev. Lett. **32**, 52 (1974); A. Rahman, Phys. Rev. A **9**, 1667 (1974).

[7]K. Carneiro, M. Nielsen, and J. P. McTague, Phys. Rev. Lett. **30**, 481 (1973).

[8]P. Bosi, F. Dupré, F. Menzinger, F. Sacchetti, and M. C. Spinelli, Lett. Nuovo Cimento **21**, 436 (1978).

[9]J. Teixeira, M. C. Bellissent-Funel, S. H. Chen, and B. Dorner,

Phys. Rev. Lett. **54**, 2681 (1985); J. Teixeira, M. C. Bellissent-Funel, S. H. Chen and B. Dorner, in *Water and Aqueous Solutions,* edited by G. W. Neilson and J. E. Enderby (Adam Hilger, Bristol, 1986).

[10]A. Rahman and F. H. Stillinger, Phys. Rev. A **10**, 368 (1978). The ST2 effective potential has been introduced for the first time by F. H. Stillinger and A. Rahman, J. Chem. Phys. **60**, 1545 (1974).

[11]R. W. Impey, P. A. Madden, and I. R. McDonald, Mol. Phys. **46**, 513 (1982).

[12]M. Wojcik and E. Clementi, J. Chem. Phys. **85**, 6085 (1986).

[13]M. A. Ricci, D. Rocca, G. Ruocco, and R. Vallauri, Phys. Rev. Lett. **61**, 1958 (1988).

[14]A. comprehensive review of the method is reported, for example, by B. J. Berne, in *Statistical Mechanics,* edited by B. J. Berne (Plenum, New York, 1977), Part B, p. 233.

[15]C. G. Gray and K. E. Gubbins, *Theory of Molecular Fluids: Fundamentals, Vol. 1* (Clarendon, Oxford, 1984).

[16]W. L. Jorgensen, J. Chandrasekhara, J. D. Madura, R. W. Impey, and M. L. Klein, J. Chem. Phys. **79**, 926 (1983).

[17]M. Ferrario and A. Tani, Chem. Phys. Lett. **121**, 182 (1985); M. Neumann, J. Chem. Phys. **85**, 1567 (1986); M. Rami Reddy and M. Berkowitz, *ibid.* **87**, 6682 (1987); J. S. Tse and M. L. Klein, J. Phys. Chem. **92**, 315 (1988); J. D. Madura, B. Montgomery Pettitt, and D. F. Calef, Mol. Phys. **64**, 325 (1988); M. A. Ricci, G. Ruocco, and M. Sampoli, Mol. Phys. **67**, 19 (1989).

[18]D. J. Evans and S. Murad, Mol. Phys. **79**, 327 (1977).

[19]N. E. Dorsey, in *Properties of Ordinary Water-Substance* (Hafner, New York, 1968).

[20]P. G. de Gennes, Physica **25**, 825 (1959).

[21]J. P. Hansen and I. R. McDonald, *Theory of Simple Liquids* (Academic, New York, 1976).

[22]The correlation functions have been followed up to $T=2.56\times10^{-11}$ s; therefore the step in the Fourier Transform turns out to be $\delta\omega=\pi/T$. This leads to a frequency resolution $\Delta=4\delta\omega\approx5\times10^{11}$ s^{-1} [see A. Papoulis, *Probability Random Variables and Stochastic Processes* (McGraw-Hill, New York, 1984)].

[23]M. Nardone and P. Benassi, Chem. Phys. Lett. **145**, 575 (1988); P. Benassi, G. D'Arrigo, and M. Nardone, J. Chem. Phys. **89**, 4469 (1988), and references therein.

[24]C. J. Montrose, J. A. Bucaro, J. Marshall-Cookley, and T. A. Litovitz, J. Chem. Phys. **60**, 5025 (1974); W. Denninger and G. Zundel, *ibid.* **74**, 2769 (1981); O. Conde and J. Teixeira, J. Phys. **44**, 525 (1983); V. Mazzacurati and P. Benassi, Chem. Phys. **112**, 147 (1987).

[25]V. Mazzacurati, M. A. Ricci, G. Ruocco, and M. Sampoli Chem. Phys. Lett. **159**, 383 (1989).

[26]L. Bosio, J. Teixeira, and H. E. Stanley, Phys. Rev. Lett. **46**, 597 (1981).

[27]J. C. Michielsen, A. Bot, and J. van der Elsken, Phys. Rev. A **38**, 6439 (1988).

[28]B. Renker, Phys. Lett. A **30**, 493 (1969); B. Renker in *Physics and Chemistry of Ice,* edited by E. Whalley, S. J. Jones, and L. W. Gold (Royal Society of Canada, Ottawa, 1973).